LULEÅ
UNIVERSITY
OF TECHNOLOGY

Division of Signal Processing
Visiting address: Universitetsområdet, Porsön, Luleå
Postal address: SE-971 87, Luleå, Sweden
Telephone: +46 920 910 00. *Fax:* +46 920 720 43
URL: http://www.sm.luth.se/csee/sp/

ML Estimation of Time and Frequency Offset in OFDM Systems

Jan-Jaap van de Beek, Magnus Sandell
and Per Ola Börjesson

In *IEEE Transactions on Signal Processing*,
vol. 45, no. 7, pp. 1800-1805, July 1997.

© 1997 IEEE. Personal use of this material is permitted.
However, permission to reprint/republish this material for advertising or promotional purposes or for creating new collective works for resale or redistribution to servers or lists, or to reuse any copyrighted component of this work in other works must be obtained from the IEEE.

ML Estimation of Time and Frequency Offset in OFDM Systems

Jan-Jaap van de Beek, *Student Member, IEEE*, Magnus Sandell, *Student Member, IEEE*, and Per Ola Börjesson, *Member, IEEE*

***Abstract*— We present the joint maximum likelihood (ML) symbol-time and carrier-frequency offset estimator in orthogonal frequency-division multiplexing (OFDM) systems. Redundant information contained within the cyclic prefix enables this estimation without additional pilots. Simulations show that the frequency estimator may be used in a tracking mode and the time estimator in an acquisition mode.**

I. Introduction

ORTHOGONAL frequency-division multiplexing (OFDM) systems have recently gained increased interest. OFDM is used in the European digital broadcast radio system and is being investigated for other wireless applications such as digital broadcast television and mobile communication systems, as well as for broadband digital communication on existing copper networks. See [1] and [2] and the references therein.

We address two problems in the design of OFDM receivers. One problem is the unknown OFDM symbol arrival time. Sensitivity to a time offset is higher in multicarrier systems than in single-carrier systems and has been discussed in [3] and [4]. A second problem is the mismatch of the oscillators in the transmitter and the receiver. The demodulation of a signal with an offset in the carrier frequency can cause a high bit error rate and may degrade the performance of a symbol synchronizer [3], [5].

A symbol clock and a frequency offset estimate may be generated at the receiver with the aid of pilot symbols known to the receiver [6], [7], or, as in [8], by maximizing the average log-likelihood function. Redundancy in the transmitted OFDM signal also offers the opportunity for synchronization. Such an approach is found in [7], [9], and [10] for a time offset and in [10]–[12] for a frequency offset. We present and evaluate the joint maximum likelihood (ML) estimation of the time and carrier-frequency offset in OFDM systems. The key element that will rule the discussion is that the OFDM data symbols already contain sufficient information to perform synchronization. Our novel algorithm exploits the cyclic prefix preceding the OFDM symbols, thus reducing the need for pilots.

Manuscript received December 1, 1996; revised January 2, 1997. The associate editor coordinating the review of this paper and approving it for publication was Prof. Giorgios B. Giannakis.

The authors are with the Division of Signal Processing and the Centre for Distance–Spanning Technology, Luleå University of Technology, Luleå, Sweden.

Publisher Item Identifier S 1053-587X(97)04946-5.

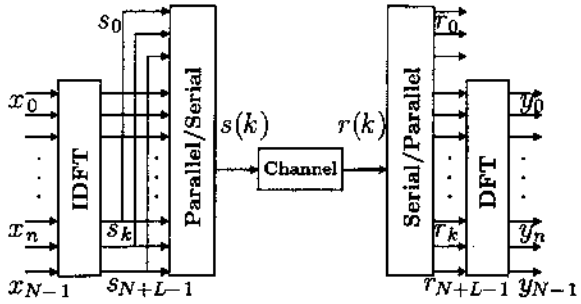

Fig. 1. OFDM system, transmitting subsequent blocks of N complex data.

II. The OFDM System Model

Fig. 1 illustrates the baseband, discrete-time OFDM system model we investigate. The complex data symbols are modulated by means of an *inverse discrete Fourier transform* (IDFT) on N-parallel subcarriers. The resulting OFDM symbol is serially transmitted over a discrete-time channel, whose impulse response we assume is shorter than L samples. At the receiver, the data are retrieved by means of a *discrete Fourier transform* (DFT).

An accepted means of avoiding intersymbol interference (ISI) and preserving orthogonality between subcarriers is to copy the last L samples of the body of the OFDM symbol (N samples long) and append them as a preamble—the cyclic prefix—to form the complete OFDM symbol [1], [2]. The effective length of the OFDM symbol as transmitted is this cyclic prefix plus the body ($L+N$ samples long). The insertion of a cyclic prefix can be shown to result in an equivalent parallel orthogonal channel structure that allows for simple channel estimation and equalization [13]. In spite of the loss of transmission power and bandwidth associated with the cyclic prefix, these properties generally motivate its use [1], [2].

In the following analysis, we assume that the channel is nondispersive and that the transmitted signal $s(k)$ is only affected by complex additive white Gaussian noise (AWGN) $n(k)$. We will, however, evaluate our estimator's performance for both the AWGN channel and a time-dispersive channel.

Consider two uncertainties in the receiver of this OFDM symbol: the uncertainty in the arrival time of the OFDM symbol (such ambiguity gives rise to a rotation of the data symbols) and the uncertainty in carrier frequency (a difference in the local oscillators in the transmitter and receiver gives rise to a shift of all the subcarriers). The first uncertainty is modeled as a delay in the channel impulse response $\delta(k-\theta)$, where

1053–587X/97$10.00 © 1997 IEEE

θ is the integer-valued unknown arrival time of a symbol. The latter is modeled as a complex multiplicative distortion of the received data in the time domain $e^{j2\pi\varepsilon k/N}$, where ε denotes the difference in the transmitter and receiver oscillators as a fraction of the intercarrier spacing ($1/N$ in normalized frequency). Notice that all subcarriers experience the same shift ε. These two uncertainties and the AWGN thus yield the received signal

$$r(k) = s(k-\theta)e^{j2\pi\varepsilon k/N} + n(k). \tag{1}$$

Two other synchronization parameters are not accounted for in this model. First, an offset in the carrier phase may affect the symbol error rate in coherent modulation. If the data is differentially encoded, however, this effect is eliminated. An offset in the sampling frequency will also affect the system performance. We assume that such an offset is negligible. The effect of nonsynchronized sampling is investigated in [14].

Now, consider the transmitted signal $s(k)$. This is the DFT of the data symbols x_k, which we assume are independent. Hence, $s(k)$ is a linear combination of independent, identically distributed random variables. If the number of subcarriers is sufficiently large, we know from the central limit theorem that $s(k)$ approximates a complex Gaussian process whose real and imaginary parts are independent. This process, however, is not white since the appearance of a cyclic prefix yields a correlation between some pairs of samples that are spaced N samples apart. Hence, $r(k)$ is not a white process either, but because of its probabilistic structure, it contains information about the time offset θ and carrier frequency offset ε. This is the crucial observation that offers the opportunity for joint estimation of these parameters based on $r(k)$.

A synchronizer cannot distinguish between phase shifts introduced by the channel and those introduced by symbol time delays [4]. Time error requirements may range from the order of one sample (wireless applications, where the channel phase is tracked and corrected by the channel equalizer) to a fraction of a sample (in, e.g., high bit-rate digital subscriber lines, where the channel is static and essentially estimated only during startup).

Without a frequency offset, the frequency response of each subchannel is zero at all other subcarrier frequencies, i.e., the subchannels do not interfere with one other [2]. The effect of a frequency offset is a loss of orthogonality between the tones. The resulting intercarrier interference (ICI) has been investigated in [11]. The effective signal-to-noise ratio (SNR_e) due to both additive noise and ICI is shown to be lower bounded by

$$\mathrm{SNR}_e(\varepsilon) \geq \frac{\mathrm{SNR}}{1 + 0.5947\,\mathrm{SNR}\,\sin^2\pi\varepsilon}\left(\frac{\sin\pi\varepsilon}{\pi\varepsilon}\right)^2 \tag{2}$$

where

$$\mathrm{SNR} = \sigma_s^2/\sigma_n^2, \sigma_s^2 \triangleq E\{|s(k)|^2\} \quad \text{and} \quad \sigma_n^2 \triangleq E\{|n(k)|^2\}.$$

The difference between the SNR and the SNR_e is a measure of the sensitivity to a frequency offset ε. Notice that in the absence of additive noise, the frequency offset must satisfy $|\varepsilon| \leq 1.3 \cdot 10^{-2}$ in order to obtain an SNR_e of 30 dB or higher. This result agrees well with the analysis of multiuser OFDM systems in [3], which states that a frequency accuracy of 1–2% of the intercarrier spacing is necessary.

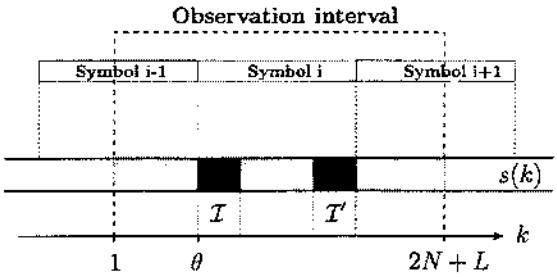

Fig. 2. Structure of OFDM signal with cyclicly extended symbols $s(k)$. The set $\mathcal{I}$ contains the cyclic prefix, i.e., the copies of the L data samples in $\mathcal{I}'$.

III. ML Estimation

Assume that we observe $2N + L$ consecutive samples of $r(k)$, cf. Fig. 2, and that these samples contain one complete $(N + L)$-sample OFDM symbol. The position of this symbol within the observed block of samples, however, is unknown because the channel delay θ is unknown to the receiver. Define the index sets

$$\mathcal{I} \triangleq \{\theta, \cdots, \theta + L - 1\} \quad \text{and}$$
$$\mathcal{I}' \triangleq \{\theta + N, \cdots, \theta + N + L - 1\}$$

(see Fig. 2). The set $\mathcal{I}'$ thus contains the indices of the data samples that are copied into the cyclic prefix, and the set $\mathcal{I}$ contains the indices of this prefix. Collect the observed samples in the $(2N+L)\times 1$-vector $\boldsymbol{r} \triangleq [r(1)\cdots r(2N+L)]^T$. Notice that the samples in the cyclic prefix and their copies $r(k), k \in \mathcal{I} \cup \mathcal{I}'$ are pairwise correlated, i.e.,

$$\forall k \in \mathcal{I}: \quad E\{r(k)r^*(k+m)\} = \begin{cases} \sigma_s^2 + \sigma_n^2 & m = 0 \\ \sigma_s^2 e^{-j2\pi\varepsilon} & m = N \\ 0 & \text{otherwise} \end{cases} \tag{3}$$

while the remaining samples $r(k), k \notin \mathcal{I} \cup \mathcal{I}'$ are mutually uncorrelated.

The log-likelihood function for θ and ε, $\Lambda(\theta, \varepsilon)$ is the logarithm of the probability density function $f(\boldsymbol{r}|\theta, \varepsilon)$ of the $2N + L$ observed samples in $\boldsymbol{r}$ given the arrival time θ and the carrier frequency offset ε. In the following, we will drop all additive and positive multiplicative constants that show up in the expression of the log-likelihood function since they do not affect the maximizing argument. Moreover, we drop the conditioning on (θ, ε) for notational clarity. Using the correlation properties of the observations $\boldsymbol{r}$, the log-likelihood function can be written as

$$\begin{aligned} \Lambda(\theta,\varepsilon) &= \log f(\boldsymbol{r}|\theta,\varepsilon) \\ &= \log\left(\prod_{k\in\mathcal{I}} f(r(k), r(k+N)) \prod_{k\notin\mathcal{I}\cup\mathcal{I}'} f(r(k))\right) \\ &= \log\left(\prod_{k\in\mathcal{I}} \frac{f(r(k), r(k+N))}{f(r(k))f(r(k+N))} \prod_{k} f(r)k))\right) \end{aligned} \tag{4}$$

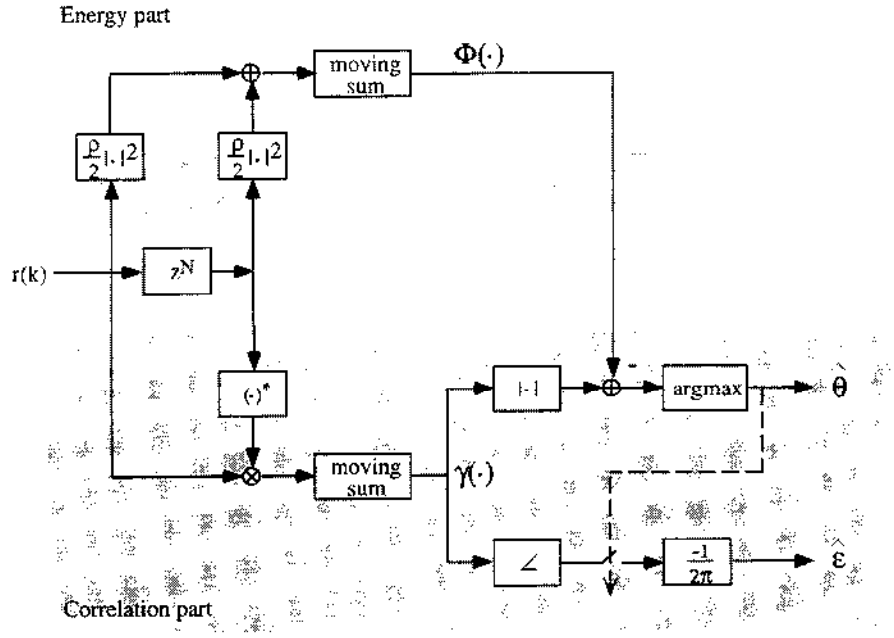

Fig. 3. Structure of the estimator.

where $f(\cdot)$ denotes the probability density function of the variables in its argument. Notice that it is used for both one- and two-dimensional (1-D and 2-D) distributions. The product $\Pi_k\ f(r(k))$ in (4) is independent of θ (since the product is over all k) and ε (since the density $f(r(k))$ is rotationally invariant). Since the ML estimation of θ and ε is the argument maximizing $\Lambda(\theta, \varepsilon)$, we may omit this factor. Under the assumption that $\boldsymbol{r}$ is a jointly Gaussian vector, (4) is shown in the Appendix to be

$$\Lambda(\theta, \varepsilon) = |\gamma(\theta)| \cos(2\pi\varepsilon + \angle\gamma(\theta)) - \rho\Phi(\theta) \tag{5}$$

where $\angle$ denotes the argument of a complex number

$$\gamma(m) \triangleq \sum_{k=m}^{m+L-1} r(k)r^*(k+N), \tag{6}$$

$$\Phi(m) \triangleq \tfrac{1}{2} \sum_{k=m}^{m+L-1} |r(k)|^2 + |r(k+N)|^2 \tag{7}$$

and

$$\rho \triangleq \left| \frac{E\{r(k)r^*(k+N)\}}{\sqrt{E\{|r(k)|^2\}E\{|r(k+N)|^2\}}} \right| = \frac{\sigma_s^2}{\sigma_s^2 + \sigma_n^2} = \frac{\mathrm{SNR}}{\mathrm{SNR}+1} \tag{8}$$

is the magnitude of the correlation coefficient between $r(k)$ and $r(k+N)$. The first term in (5) is the weighted magnitude of $\gamma(\theta)$, which is a sum of L consecutive correlations between pairs of samples spaced N samples apart. The weighting factor depends on the frequency offset. The term $\Phi(\theta)$ is an energy term, independent of the frequency offset ε. Notice that its contribution depends on the SNR (by the weighting-factor ρ).

The maximization of the log-likelihood function can be performed in two steps:

$$\max_{(\theta,\varepsilon)} \Lambda(\theta, \varepsilon) = \max_{\theta} \max_{\varepsilon} \Lambda(\theta, \varepsilon) = \max_{\theta} \Lambda(\theta, \hat{\varepsilon}_{\mathrm{ML}}(\theta)). \tag{9}$$

The maximum with respect to the frequency offset ε is obtained when the cosine term in (5) equals one. This yields the ML estimation of ε

$$\hat{\varepsilon}_{\mathrm{ML}}(\theta) = -\frac{1}{2\pi}\angle\gamma(\theta) + n \tag{10}$$

where n is an integer. A similar frequency offset estimator has been derived in [11] under different assumptions. Notice that by the periodicity of the cosine function, several maxima are found. We assume that an acquisition, or rough estimate, of the frequency offset has been performed and that $|\varepsilon| < 1/2$; thus, $n = 0$. Since $\cos(2\pi\hat{\varepsilon}_{\mathrm{ML}}(\theta + \angle\gamma(\theta)) = 1$, the log-likelihood function of θ (which is the compressed log-likelihood function with respect to ε) becomes

$$\Lambda(\theta, \hat{\varepsilon}_{\mathrm{ML}}(\theta)) = |\gamma(\theta)| - \rho\Phi(\theta) \tag{11}$$

and the joint ML estimation of θ and ε becomes

$$\hat{\theta}_{\mathrm{ML}} = \arg \max_{\theta} \{|\gamma(\theta)| - \rho\Phi(\theta)\} \tag{12}$$

$$\hat{\varepsilon}_{\mathrm{ML}} = -\frac{1}{2\pi}\angle\gamma(\hat{\theta}_{\mathrm{ML}}). \tag{13}$$

Notice that only two quantities affect the log-likelihood function (and thus the performance of the estimator): the number of samples in the cyclic prefix L and the correlation coefficient ρ given by the SNR. The former is known at the receiver, and the latter can be fixed. Basically, the quantity $\gamma(\theta)$ provides the estimates of θ and ε. Its magnitude, which is compensated by an energy term, peaks at time instant $\hat{\theta}_{\mathrm{ML}}$,

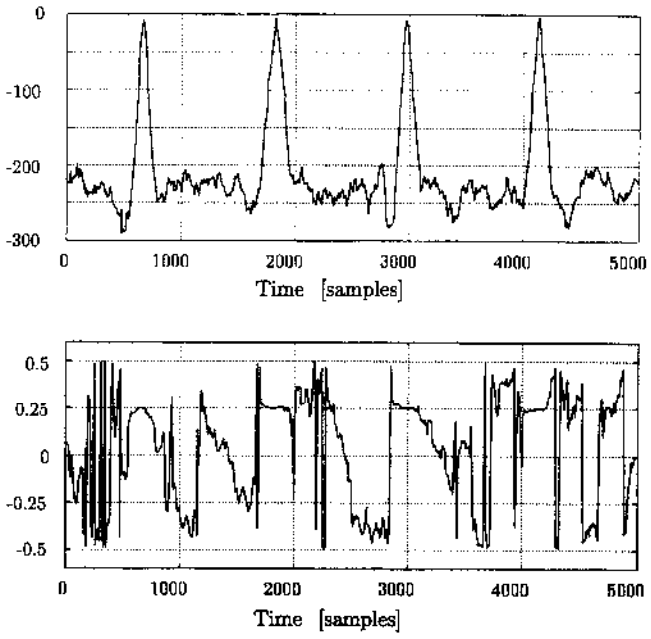

Fig. 4. Signals that generate the ML estimates ($N = 1024, L = 128$, $\varepsilon = 0.25$, and SNR = 15 dB): The maximizing indices of $\Lambda(\theta, \hat{\varepsilon}_{\mathrm{ML}}(\theta))$ (top) yield the time estimates $\hat{\theta}_{\mathrm{ML}}$. At these time instants the arguments of $\gamma(\theta)$ (bottom) yield $\hat{\varepsilon}_{\mathrm{ML}}$.

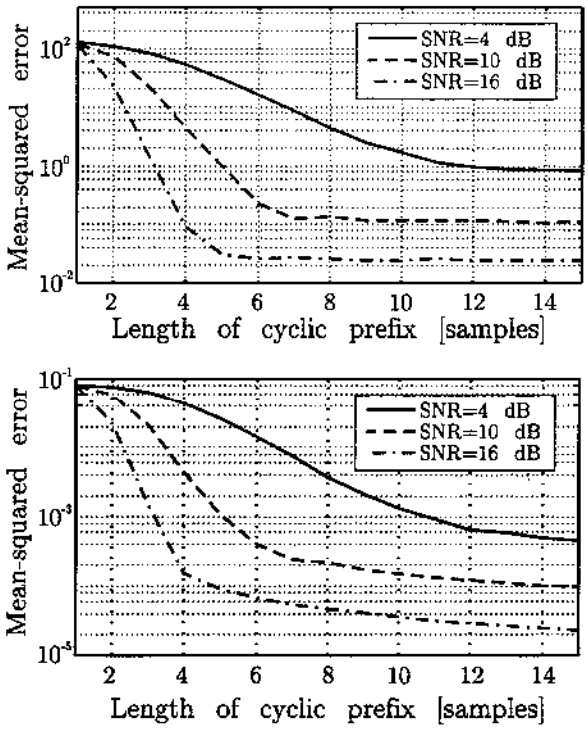

Fig. 5. Performance of the time (top) and frequency (bottom) estimators for the AWGN channel (4, 10, and 16 dB). The dimensionless performance measure is expressed in squared units relative to the sample interval (top) and the intertone spacing (bottom). The number of subcarriers is $N = 256$.

while its phase at this time instant is proportional to $\hat{\varepsilon}_{\mathrm{ML}}$. If ε is *a priori* known to be zero, the log-likelihood function for θ becomes $\Lambda(\theta) = \mathrm{Re}\{\gamma(\theta)\} - \rho\Phi(\theta)$, and $\hat{\theta}_{\mathrm{ML}}$ is its maximizing argument. This estimator and a low-complexity variant are analyzed in [9].

In an OFDM receiver, the quantity $\gamma(\theta)$, which is defined in (6), is calculated on-line, cf. Fig. 3. The signals $\Lambda(\theta, \hat{\varepsilon}_{\mathrm{ML}}(\theta))$ (whose maximizing arguments are the time estimates $\hat{\theta}_{\mathrm{ML}}$) and $-(1/2\pi)\angle\gamma(\theta)$ (whose values at the time instants $\hat{\theta}_{\mathrm{ML}}$ yield the frequency estimates) are shown in Fig. 4. Notice that (12) and (13) describe an open-loop structure. Closed-loop implementations based on (5) and (11) may also be considered. In such structures, the signal $\Lambda(\theta, \hat{\varepsilon}_{\mathrm{ML}}(\theta))$ is typically fed back in a phase-locked loop (PLL). If we can assume that θ is constant over a certain period, the integration in the PLL can significantly improve the performance of the estimators.

IV. Simulations

We use Monte Carlo simulations to evaluate the performance of the estimators in which we consider an OFDM system with 256 subcarriers. In each simulation, 125 000 symbols are used. We evaluate the performance of the estimators by means of the estimator mean-squared error.

Performance results for the AWGN channel are shown in Figs. 5 and 6. First, the estimator mean-squared error as a function of L is estimated. Fig. 5 shows the estimator performance for SNR values of 4, 10, and 16 dB. Notice that the performance of the time estimator is asymptotically independent of L, provided that the cyclic prefix is longer than a certain threshold value. This threshold value decreases with the SNR. Both the time and the frequency estimator exhibit such a performance threshold based on L. However, notice that as L increases beyond these respective thresholds, only the frequency estimator will show continued improvement. Thus, for the AWGN channel and from a time synchronization viewpoint, there is very little advantage in increasing the length of the cyclic prefix beyond the time estimator's threshold.

Second, the estimator variances as a function of SNR for $L = 4, L = 8$, and $L = 15$ are shown in Fig. 6. Notice that even in these plots, a threshold phenomenon as in Fig. 5 occurs. This phenomenon is a property of time delay estimation and is documented in, e.g., [15].

The above results do not directly apply to a time-dispersive channel environment. Therefore, we also consider the performance of our estimators in a wireless system operating at 2 GHz with a bandwidth of 5 MHz. An outdoor dispersive, fading environment with microcell characteristics is chosen: The channel has an exponentially decaying power delay profile with root mean squared width equal to 0.4 μs (corresponding to two samples) and a maximum delay spread of 3 μs (corresponding to 15 samples). It is modeled to consist of 15 independent Rayleigh-fading taps [16] and additive noise. We choose a cyclic prefix consisting of 15 samples. This choice avoids ISI, whereas the loss of power and bandwidth due to the cyclic prefix $(L/(N+L))$ is about 5%. This system transmits about 18 000 OFDM symbols per second, each containing 256 complex information symbols. In this dispersive environment, the definition of θ is ambigious. We define the true delay as the center of gravity of the channel impulse response. Moreover, we define the SNR as $\mathrm{SNR} = \sigma_s^2 P_h / \sigma_n^2$, where P_h is the sum of the average power in all channel taps.

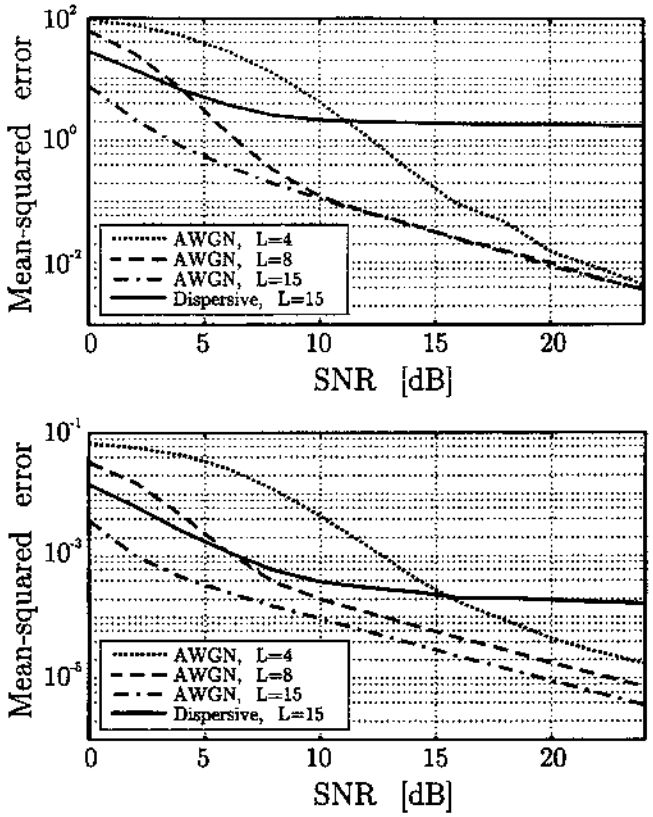

Fig. 6. Performance of the time (top) and frequency (bottom) estimators for the AWGN channel ($L = 4$, $L = 8$, and $L = 15$) and the dispersive channel ($L = 15$). The dimensionless performance measure is expressed in squared units relative to the sample interval (top) and the inter-tone spacing (bottom). The number of subcarriers is $N = 256$.

The error floor in Fig. 6 clearly shows the performance degradation caused by the dispersive channel as compared with the corresponding curves for the AWGN channel. In the dispersive case, the estimators operate in an environment for which they are not designed (they are not optimal). Signals passed through the AWGN channel will have the simple, pairwise correlation structure (3), but signals passed through a dispersive channel generally have a more complex correlation structure.

Depending on the application and the presence of a high-performance channel estimator/equalizer, the performance of the time estimate in Fig. 6 (standard deviation of 1–2 samples) may be good enough to generate a stable clock. In most situations, this performance will suffice at least in an acquisition mode. The frequency offset estimator shows an error standard deviation of less than 2% of the intertone spacing (see Fig. 6), which satisfies the requirements discussed in Section II.

Finally, the performance of the frequency estimator is plotted in Fig. 7 by means of the SNR loss in decibels: SNR_ε-SNR. The SNR loss is [*cf.* (2)] a function of ε. We assume that a frequency offset can be corrected using the estimate $\hat{\varepsilon}_{\text{ML}}$, and we thus use the standard deviation of the estimate as the argument in (2). The SNR loss is plotted for the AWGN channel and the dispersive channel. Notice that even for the dispersive channel, this loss does not exceed 0.5 dB for SNR values between 0 and 20 dB.

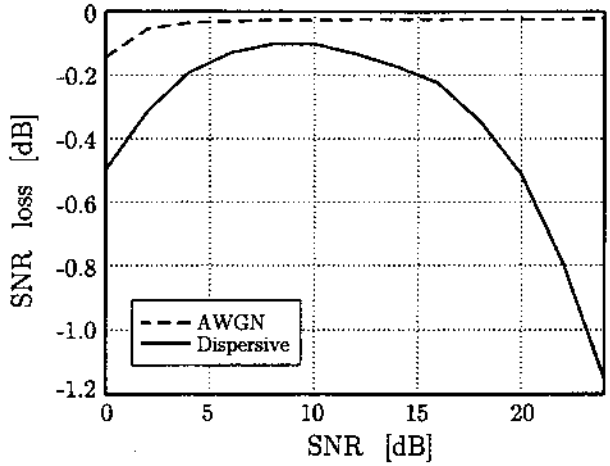

Fig. 7. Performance of the frequency estimator for the AWGN channel and the dispersive channel ($L = 15$). The number of subcarriers is $N = 256$.

V. Discussion

We have presented the joint ML estimator of time and frequency offset in OFDM systems. It uses the redundant information contained within the cyclic prefix. It is derived under the assumption that the channel distortion only consists of additive noise, but simulations show that it can perform well even in a dispersive channel. The ML estimator for the latter case may be derived, but it will not have the same simple structure as our proposed estimator.

The frequency estimator performs better than the time estimator because of its implicit averaging. From (6) and (10), the estimate is the argument of a sum of complex numbers. Without additive noise $n(k)$, each term $r(k)r^*(k+N)$ has the same argument $-2\pi\varepsilon$. Hence, they contribute coherently to the sum, whereas the additive noise contributes incoherently. This explains why the performance will improve as the size of the cyclic prefix increases.

In wireless systems, pilots are needed for channel estimation. These pilots can be used by the synchronizer in order to further increase performance. Resulting synchronizers may be hybrid structures using both pilots and the redundancy of the cyclic prefix. How to incorporate pilot symbols in such time and frequency estimators is not straightforward and needs further research.

Appendix
The Log-Likelihood Function

The log-likelihood function (4) can be written as

$$\Lambda(\theta,\varepsilon) = \sum_{k=\theta}^{\theta+L-1} \log\left(\frac{f(r(k), r(k+N))}{f(r(k))f(r(k+N))}\right). \qquad (14)$$

The numerator is a 2-D complex-valued Gaussian distribution, which, using the correlation properties (3), becomes (15), shown at the top of the next page, where ρ is the magnitude of the correlation coefficient between $r(k)$ and $r(k+N)$ as defined in (8). The denominator of (14) consists of two 1-D

$$f(r(k), r(k+N)) = \frac{\exp\left(-\dfrac{|r(k).^2 - 2\rho\,\mathrm{Re}\{e^{j2\pi\varepsilon} r(k) r^*(k+N)\} + |r(k+N)|^2}{(\sigma_s^2+\sigma_n^2)(1-\rho^2)}\right)}{\pi^2(\sigma_s^2+\sigma_n^2)^2(1-\rho^2)} \tag{15}$$

complex Gaussian distributions

$$f(r(k)) = \frac{\exp\left(-\dfrac{|r(k)|^2}{(\sigma_s^2+\sigma_n^2)}\right)}{\pi(\sigma_s^2+\sigma_n^2)} \tag{16}$$

and the log-likelihood function (14), after some algebraic manipulations, becomes

$$\Lambda(\theta,\varepsilon) = c_1 + c_2(|\gamma(\theta)|\cos(2\pi\varepsilon + \angle\gamma(\theta)) - \rho\Phi(\theta)) \tag{17}$$

where $\gamma(m)$ and $\Phi(m)$ are defined in (6) and (7), and c_1 and c_2 are constants, independent of θ and ε. Since the maximizing argument of $\Lambda(\theta,\varepsilon)$ is independent of the constants c_1 and c_2, and $c_2 > 0$, the ML-estimate $(\hat{\theta}_{\mathrm{ML}}, \hat{\varepsilon}_{\mathrm{ML}})$ also maximizes (5).

ACKNOWLEDGMENT

The authors wish to thank M. Isaksson, Telia Research AB, Luleå, Sweden, for many stimulating discussions during the early stages of the project leading to this paper.

REFERENCES

[1] W. Y. Zou, and Y. Wu, "COFDM: An overview," *IEEE Trans. Broadcasting*, vol. 41, pp. 1–8, Mar. 1995.
[2] J. A. C. Bingham, "Multicarrier modulation for data transmission: An idea whose time has come," *IEEE Commun. Mag.*, vol. 28, pp. 5–14, May 1990.
[3] L. Wei and C. Schlegel, "Synchronization requirements for multi-user OFDM on satellite mobile and two-path Rayleigh fading channels," *IEEE Trans. Commun.*, vol. 43, pp. 887–895, Feb./Mar./Apr. 1995.
[4] T. Pollet and M. Moeneclaey, "Synchronizability of OFDM signals," in *Proc. Globecom'95*, Singapore, vol. 3, Nov. 1995, pp. 2054–2058.
[5] T. Pollet, M. van Bladel, and M. Moeneclaey, "BER sensitivity of OFDM systems to carrier frequency offset and Wiener phase noise," *IEEE Trans. Commun.*, vol. 43, pp. 191–193, Feb./Mar./Apr. 1995.
[6] W. D. Warner and C. Leung, "OFDM/FM frame synchronization for mobile radio data communication," *IEEE Trans. Veh. Technol.*, vol. 42, pp. 302–313, Aug. 1993.
[7] P. J. Tourtier, R. Monnier, and P. Lopez, "Multicarrier modem for digital HDTV terrestrial broadcasting," *Signal Processing: Image Commun.*, vol. 5, no. 5–6, pp. 379–403, Dec. 1993.
[8] F. Daffara and A. Chouly, "Maximum likelihood frequency detectors for orthogonal multicarrier systems," in *Proc. IEEE Int. Conf. Commun.*, May 1993, pp. 766–771.
[9] J. J. van de Beek, M. Sandell, M. Isaksson, and P. O. Börjesson, "Low-complex frame synchronization in OFDM systems," in *Proc. IEEE Int. Conf. Universal Personal Commun.*, Nov. 1995, pp. 982–986.
[10] M. Sandell, J. J. van de Beek, and P. O. Börjesson, "Timing and frequency synchronization in OFDM systems using the cyclic prefix," in *Proc. IEEE Int. Symp. Synchronization*, Essen, Germany, Dec. 1995, pp. 16–19.
[11] P. H. Moose, "A technique for orthogonal frequency division multiplexing frequency offset correction," *IEEE Trans. Commun.*, vol. 42, pp. 2908–2914, Oct. 1994.
[12] F. Daffara and O. Adami, "A new frequency detector for orthogonal multicarrier transmission techniques," in *Proc. Vehic. Technol. Conf.*, Chicago, IL, vol. 2, July 1995, pp. 804–809.
[13] A. Peled and A. Ruiz, "Frequency domain data transmission using reduced computational complexity algorithms," in *Proc. IEEE ICASSP*, Denver, CO, 1980, pp. 964–967.
[14] T. Pollet, P. Spruyt, and M. Moeneclaey, "The BER performance of OFDM systems using non-synchronized sampling," in *Proc. IEEE Globecom.*, San Francisco, CA, vol. I, Nov. 1994, pp. 253–257.
[15] G. C. Carter, "Coherence and time delay estimation," *Proc. IEEE*, vol. 75, pp. 236–255, Feb. 1987.
[16] W. C. Jakes, *Microwave Mobile Communications*. New York: IEEE, 1974, classic reissue.

Jan-Jaap van de Beek (S'96) was born in Alphen aan den Rijn, The Netherlands, in 1967. He received the M.Sc. degree in applied mathematics from the University of Twente, Twente, The Netherlands, in 1992. In 1996, he received the Lic. Eng. degree in signal processing from Luleå University of Technology, Luleå, Sweden, where he is currently working toward the Ph.D. degree at the Division of Signal Processing.

His research interests include statistical parameter estimation in multicarrier communication systems and biomedical engineering.

Magnus Sandell (S'95) was born in Eksjö, Sweden, in 1965. He received the M.Sc. degree in electrical engineering in 1990 and the Ph.D. degree in signal processing in 1996, both from Luleå University of Technology, Luleå, Sweden. He is currently working as a researcher at the Division of Signal Processing at the same university.

His research interests include estimation problems and multidimensional signal processing with applications in telecommunications and biomedical engineering.

Per Ola Börjesson (M'80) was born in Karlshamn, Sweden, in 1945. He received the M.Sc. degree in electrical engineering in 1970 and the Ph.D. degree in telecommunication theory in 1980, both from Lund Institute of Technology (LTH), Lund, Sweden. In 1983, he received the degree of Docent in Telecommunication Theory.

Since 1988, he has been Professor of Signal Processing at Luleå University of Technology, Luleå, Sweden. His primary research interest is in high-performance communication systems, in particular, high data rate wireless and twisted pair systems. He is presently researching signal processing techniques in communiation systems that use orthogonal frequency division multiplexing (OFDM) or discrete multitone (DMT) modulation. He emphasizes the interaction between models and real systems from the creation of application-oriented models based on system knowledge to the implementation and evaluation of algorithms.